اولین کنفرانس احتراق ایران
بهمن ماه ۱۳۸۴ - تهران- دانشگاه تربیت مدرس
انجمن احتراق ایران

Numerical Modeling and Investigation of Candle Flame under Different Ambient Pressures

Bahman Abbasi[1], Reza Ebrahimi[2], Shafagh Tavasoli[3]
Mechanical Engineering Department, K.N.T. University of Technology
Bahman_Abbasi@kntu.ac.ir

Abstract
Laminar candle flame is modeled and studied by numerical methods. A candle with a specific geometry is placed in an enclosure and is subjected to atmospheric conditions. As the candle is ignited, a diffusion flame forms, grows and affects the ambient temperature, pressure and causes natural convection at the proximity of the flame. Equations and methods to evaluate material properties accurately in case of severe dependence of results on material properties are developed and reported. Equations governing the problem are introduced and adapted for the present case. Effect of different ambient pressures on the flame characteristics and soot is examined and discussed. Qualitative comparison of results shows good agreement with theory and experiment. Results are employed to explain and reason the effects of various parameters on the flame and to get a deep insight into fundamentals of laminar diffusion flames.

Key words: Candle, n-eicosane, combustion, laminar diffusion flame, soot.

1- Introduction
Candle flame has been subject of extensive experiments for centuries. In 1965, effect of pressure on the candle flame was reported in [1]. Later, in 1969, the candle-form n-eicosane (which is the most popular material for candles) was burned to investigate species distribution above the flame and to measure the liquid surface temperature [2]. Other experiments have also been carried out to measure burning velocity (which has been awkward to determine for years [3]) and heat of combustion of the candle.

However, recently less attention has been paid to analyze candle flame with the common numerical methods and fundamental characteristics and behavior of candle flames have not been investigated comprehensively. This research aims to model the candle flame numerically and explore details of the flame under various ambient pressures. Qualitative validation and reasoning the results are then made according to previous works and physical aspects of the combustion process.

Combustion reaction is extremely sensitive to reactants and products properties; therefore, material properties are set as close as possible to real values. Standard methods employed to model temperature dependency of material properties (diffusion coefficients, thermal conductivities, heat capacities, viscosities and densities). In low speed diffusion flames, effects of radiation and thermal diffusion can be disregarded (these effects become important only in extreme cases) [4]. Basic equations governing combustion process and flow pattern model are introduced and discussed. Soot emission from flames is a very important phenomenon that must be considered in combustion analysis; hence a soot emission model in flames is described and is used to model soot emitted from the candle. Since equations governing combustion problems are usually highly stiff ones, choosing appropriate boundary conditions and numerical models and methods are of crucial importance. To bring about solution of mentioned set of equations, FLUENT (a commercial CFD program) is used.

Effects of operating conditions on properties of the flame (flame height, width, temperature and emitted soot) are investigated and reported.

2- Reaction Model and Material Properties
The materials of which candles are manufactured from are various. But typically, paraffin (alkane) with 20 carbon atoms is used to produce candles ($C_{20}H_{42}$, n-eicosane) with some additives [5, 6]. When the wick is subjected to enough temperature, n-eicosane melts, evaporates and diffuses into surrounding air. As the activation energy of $C_{20}H_{42}$ is supplied and at the presence of sufficient oxygen, the reactants burn and produce CO_2 and H_2O (as every hydrocarbon does). There are other products from this reaction that their formation and fraction depend on the reaction conditions (CO, solid carbon, etc). This process results in a diffusion flame, since reactants do not really come into contact or just have slight contact and there is a surface at which

1 MS student in Mechanical Engineering, K.N.T. University of Technology, Tehran, Iran
2 Assistant Professor, Aerospace Engineering Department, K.N.T. University of Technology, Tehran, Iran
3 BS student in Mechanical Engineering, Iran University of Science and Technology, Tehran, Iran

concentration of both reactants go to zero. This surface is known as "flame front" or "flame sheet" in diffusion flames.

To be able to model this flame, properties of the species must be reviewed at first. For Thermo-chemical properties of n-eicosane are listed in table 1 (other species' properties are easily obtained form references)

Table 1- Thermo-chemical properties of n-eicosane in atmospheric conditions [7]

Molecular weight (kg/kmole)	282.553	**Critical temperature (K)**	768
Melting point (°C)	36.4	**Ideal gas entropy of formation (J/kmole-K)**	9.3787e5
Boiling point (°C)	344	**Standard net enthalpy of combustion (J/kmole)**	-1.2391e8
Vapor density (air=1)	9.5	**Standard Gibbs enthalpy of formation (J/kmole)**	1.1570e8
Critical pressure (Pa)	1.17e6	**Ideal gas enthalpy of formation (J/kmole)**	-4.5646e8

2-1- Reaction Model and Parameters

Several reaction mechanisms are developed for hydrocarbons combustion. In this research, a single-step mechanism is used for $C_{20}H_{42}$ combustion with oxygen which is known to be a good engineering approximation [8],

$$C_xH_y + (x+\tfrac{1}{4}y)O_2 \rightarrow xCO_2 + (\tfrac{1}{2}y)H_2O \quad (1)$$

and that rate expression is,

$$\frac{d[C_xH_y]}{dt} = -A\exp(-\frac{E_a}{R_uT})[C_xH_y]^m[O_2]^n \quad (2)$$

where A is Arrhenius reaction rate equation pre-exponent factor, E_a is activation energy, R_u is universal gas constant, T is temperature of the reactants and m and n are empirical rate coefficients. For n-eicosane,

$$C_{20}H_{42} + 30.5O_2 \rightarrow 20CO_2 + 21H_2O \quad (3)$$

Four coefficients (A, E_a, m and n) should be approximated for this reaction. The values of these parameters are given in [8] for alkanes with 1 atom to 10 carbon atoms (table 2).

Table 2- Reaction rate coefficients for alkanes [8]

	C_2H_4	C_3H_8	C_4H_{10}	C_5H_{12}	C_6H_{14}	C_7H_{16}	C_8H_{18}	C_9H_{20}	$C_{10}H_{22}$
A	6.186e9	4.836e9	4.161e9	3.599e9	3.205e9	2.868e9	2.587e9	2.362e9	2.137e9
E_a **≈ (J/kmole)**	1.255e8	1.255e8	1.255e8	1.255e8	1.255e8	1.255e8	1.255e8	1.255e8	1.255e8
m	0.1	0.1	0.15	0.25	0.25	0.25	0.25	0.25	0.25
n	1.65	1.65	1.6	1.5	1.5	1.5	1.5	1.5	1.5

For the pre-exponent factor, A, an approximation should be made by use of given values. In figure 1, the available values for A are plotted against number of carbon atoms in the alkanes.

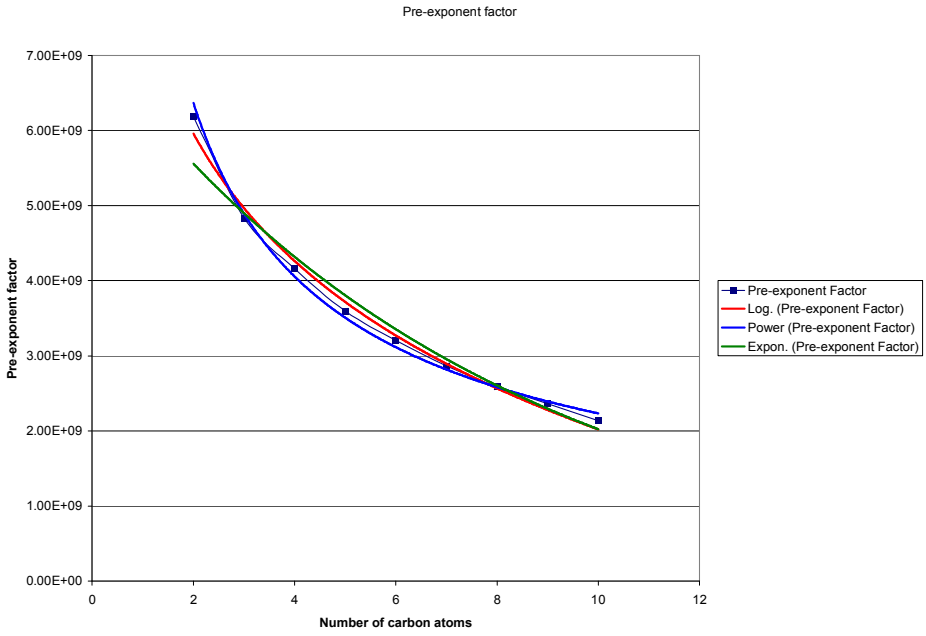

Figure 1- Pre-exponent factor as a function of carbon atoms in alkanes, three curves are fitted to estimate the value of A for the paraffin of interest

Three curves (power, exponential and logarithmic) are fitted on these points and the value of A for n-eicosane is approximated by extrapolation. A mean value regarding three curves maximum error is then obtained and substituted in equation 7,

$$\text{Power}: \quad A = 9.9996N^{-0.65083} + O(-4) \quad \Rightarrow A_{C_{20}H_{42}} = 1.4231e9 \tag{4}$$

$$\text{Exponential}: A = 7.15752\exp(-0.1263N) + O(-3) \quad \Rightarrow A_{C_{20}H_{42}} = 0.5720e9 \tag{5}$$

$$\text{Logarithmic}: A = 7.6558 - 2.4471\ln N + O(-2) \quad \Rightarrow A_{C_{20}H_{42}} = 0.3252e9 \tag{6}$$

and from these expressions,

$$A_{C_{20}H_{42}} = \frac{1}{9}[2(0.3252e9) + 3(0.5720e9) + 4(1.4231e9)] = 8.9540e8 \tag{7}$$

From table 1 it can be concluded that values 1.255e8, 0.25 and 1.5 for E_a, m, and n respectively, are suitable.

2-2- Diffusivity

As aforementioned, in the candle flame fuel diffuses into air; therefore, defining molecular diffusion factors for the reactive system is extremely important. Especially, regarding the very high temperature gradient at the proximity of the flame, diffusivity values should be temperature dependent. A standard expression for determination of diffusivity forair -hydrocarbon and non-hydrocarbon mixtures is reported in [7]. At the local temperature T (K) and total pressure P (Pa) the diffusivity of a binary system is

$$D_{12} = \frac{0.01013T^{1.75}\left(\frac{1}{M_1} + \frac{1}{M_2}\right)^{0.5}}{P[(\sum \nu_1)^{\frac{1}{3}} + (\sum \nu_2)^{\frac{1}{3}}]^2} \tag{8}$$

where D_{12} is molecular diffusivity for the binary system in m^2/sec, M is molecular weight of the component and ν is atomic diffusion volume for each component and is determined from table 3. For $C_{20}H_{42}$ the values for ν are summed over atoms.

Table 3- Atomic diffusion volumes for use in equation 8 [7]

	C	H	O_2	CO_2	H_2O	N_2
ν	16.5	1.98	16.6	26.9	12.7	17.9

In order to introduce properties to FLUENT, they must be converted into polynomials. For this reason, the values of diffusivity for each pair of species are estimated in 1atm (101325Pa) and different temperatures, then a polynomial is fitted on the points. Results of this procedure for all of the species in the mixture are tabulated below.

Table 4- Diffusivity values for binary systems in different temperatures and polynomial fitting (m^2/s)

	Diffusivity				$D_{12} = c_1 + c_2T + c_3T^2 + c_4T^3$			
Temperature (K)	**298.15**	**800**	**1200**	**1600**	C_1	C_2	C_3	C_4
$C_{20}H_{42}$-O_2	3.9879e-6	2.2439e-5	4.5622e-5	7.5447e-5	-1.542e-6	1.1593e-8	2.2837e-11	0
$C_{20}H_{42}$-CO_2	3.1700e-6	1.7838e-5	3.6266e-5	5.9998e-5	-1.484e-6	9.9887e-9	1.7795e-11	0
$C_{20}H_{42}$-H_2O	5.4307e-6	3.0558e-5	6.2128e-5	1.0279e-4	-2.542e-6	1.7108e-8	3.0487e-11	0
$C_{20}H_{42}$-N_2	4.1816e-6	2.3529e-5	4.7838e-5	7.9144e-5	-1.956e-6	1.3170e-8	2.3476e-11	0
O_2-CO_2	1.6142e-5	9.0831e-5	1.8467e-4	3.0552e-4	-7.194e-6	5.0827e-8	9.0467e-11	0
O_2-H_2O	2.2175e-4	1.2478e-3	2.5368e-3	4.1969e-3	-4.395e-5	4.3049e-7	1.5647e-09	-1.124e-13
O_2-N_2	2.0723e-5	1.1661e-4	2.3708e-4	3.9222e-4	-9.240e-6	6.5268e-8	1.1613e-10	0
CO_2-H_2O	2.1055e-5	1.1848e-4	2.4087e-4	3.9850e-4	-9.385e-6	6.6302e-8	1.1799e-10	0
CO_2-N_2	1.6407e-5	9.2323e-5	1.8770e-4	3.1054e-4	-7.315e-6	5.1669e-8	9.1949e-11	0
H_2O-N_2	2.6364e-5	1.4835e-4	3.0161e-4	4.9898e-4	-1.175e-5	8.3039e-8	1.4773e-10	0

2-3- Vapor Viscosity

For pure hydrocarbons at low pressures (P_r below 0.6), one of the most accurate models to evaluate vapor viscosity is reported in [7].

$$\mu = 4.60\times10^{-4}\frac{NM^{\frac{1}{2}}P_c^{\frac{2}{3}}}{T_c^{\frac{1}{5}}}$$

$$T_r \le 1.5 \Rightarrow N = 0.0003400T_r^{0.94} \tag{9}$$

$$T_r > 1.5 \Rightarrow N = 0.0001778(4.58T_r - 1.67)^{0.625}$$

in this equation T_c and P_c are critical temperature and pressure respectively and the resultant viscosity is in mPa.sec. Again to obtain a polynomial, the values for viscosity should be determined at different temperatures; temperatures of 800, 1000, 1152 (which corresponds to T_r = 1.5), 1200 and 1400K are used to calculate required points for polynomial fitting.

For other species, coefficients for viscosity polynomial are available. These coefficients are summarized in table 5.

Table 5- Polynomials for estimation of viscosity[4] (kg/m-sec)

	$\mu = c_1 + c_2T + c_3T^2 + c_4T^3 + c_5T^4$				
	C_1	C_2	C_3	C_4	C_5
$C_{20}H_{42}$	1.1501e-8	1.3485e-8	-8.4150e-13	-3.1740e-16	0
O_2	7.879426e-06	4.924946e-08	-9.851545e-12	1.527411e-15	-9.425674e-20
CO_2	1.9250e-6	4.3548e-8	0	0	0
H_2O	-4.418944e-06	4.687638e-08	-5.389431e-12	3.202856e-16	4.919179e-22
N_2	7.473306e-06	4.083689e-08	-8.244628e-12	1.305629e-15	-8.177936e-20

2-4- Heat Capacity

The polynomial coefficients for heat capacities for oxygen, nitrogen, water vapor and carbon dioxide are available in references. For n-eicosane, however, the coefficients are available in following format [7],

$$c_p = c_1 + c_2\left[(\frac{c_3}{T})/\sinh(\frac{c_3}{T})\right]^2 + c_4\left[(\frac{c_5}{T})/\cosh(\frac{c_5}{T})\right]^2 \quad (10)$$

wherein, c_1=3.2481e5, c_2=11.0900e5, c_3=1.1636e3, c_4=7.4500e5, c_5=-726.27. Heat capacity polynomial coefficients for the species are reported in table 6.

Table 6-Heat capacity coefficients (j/kg-K)

	$c_p = c_1 + c_2T + c_3T^2 + c_4T^3 + c_5T^4 + c_6T^5 + c_7T^6$					
	C_1	C_2	C_3	C_4	C_5	C_6
$C_{20}H_{42}$	5.66796e1	6.08400	-2.802e-3	4.1626e-7	0	0
O_2	8.76317e2	1.22828e-1	5.58304e-4	-1.20248e-6	1.14741e-9	-5.12337e-13
CO_2	5.35446e2	1.27867	-5.46776e-4	-2.38224e-7	1.89204e-10	0
H_2O	1.93780e3	-1.18077	3.64357e-3	-2.86327e-6	7.59578e-10	0
N_2	1.02705e3	2.16182e-2	1.48638e-4	-4.48421e-8	0	0

2-5- Thermal Conductivity

Likewise heat capacity coefficients, thermal conductivity coefficients are available in references. But in order to calculate thermal conductivity coefficients for the fuel and CO_2, empirical relations presented in [7] are employed.

For non-hydrocarbon linear molecules,

$$k_G = \frac{\mu_G}{M}(1.30C_v + 14644.0 - \frac{2928.8}{T_r}) \quad (11)$$

where, k_G is gas thermal conductivity (W/m-K), μ_G is vapor viscosity, C_v is specific heat in constant volume and T_r is reduced temperature. From thermodynamic tables it is found that for CO_2, T_c=304.1K and from previous sections, $\mu_{G,CO2}$=1.925e-6+4.3548e-8T and for C_v we have: C_v=Mc_p-R_u. Substituting the values for c_p, this equation leads to a function that a polynomial can be fitted on it (this procedure is already explained).

For hydrocarbons at any temperature, following equation predicts thermal conductivity [7],

$$k_G = 10^{-7}(14.52T_r - 5.14)^{\frac{2}{3}}\frac{C_p}{\lambda}$$
$$\lambda = T_c^{\frac{1}{6}}M^{\frac{1}{2}}(\frac{101325}{P_c})^{\frac{2}{3}} \quad (12)$$

where, P_c is critical pressure and its value for n-eicosane is 1.17e6Pa. Again the values of thermal conductivity are calculated at selected temperatures and a polynomial is fitted on resultant points.

Thermal conductivity coefficients are summarized in table 7.

4 References of which coefficients are reported are as follows: C20H42 and CO2 from [5]; O2, H2O and N2 are from default values available in FLUENT.

Table 7- Thermal conductivity coefficients (W/m-K)

	$k_G = c_1 + c_2T + c_3T^2 + c_4T^3 + c_5T^4$				
	C_1	C_2	C_3	C_4	C_5
$C_{20}H_{42}$	-2.7815e-2	1.0321e-4	-1.3087e-08	0	0
O_2	3.9217e-3	8.081213e-05	-1.354094e-08	2.220444e-12	-1.416139e-16
CO_2	2.5531e-2	-1.1240e-4	3.5504e-05	-2.612e-10	6.9367e-14
H_2O	-7.9679e-3	6.881332e-05	4.49046e-08	-9.099937e-12	-9.099937e-12
N_2	4.7371e-3	7.271938e-05	-1.122018e-08	1.454901e-12	-7.871726e-17

3- Governing Equations

The equations which govern behavior of reactive flows are available in literature. These equations form a highly stiff system of equations that should be solved implicitly. For this purpose the candle laminar flame is assumed to fulfill the following conditions [1]:

1- It is a steady state system, so all macroscopic variables at any point in the flame zone are independent of time.
2- The process is essentially constant pressure.
3- The reciprocal thermal diffusion (Dufour effect) is neglected.

In the proceeding sections, equations and relations that govern diffusion flame physics, flow model and soot prediction model are reviewed.

3-1- Basic Flame Equations

With above restrictions, the equations governing the behavior of laminar flame will now be summarized in general form [1].

- Overall conservation of mass: This equation states that the divergence of the total flux of matter is zero at any point.

$$\vec{\nabla}.(\rho\vec{v}) = 0 \tag{13}$$

- Conservation of a particular species: This equation states that the divergence of the flux of species *i* at any point must be equal to its net rate of appearance and disappearance due to chemical reaction, K_i. The presence of the diffusion velocity, V_i, accounts for the effect of a concentration gradient on the total flux.

$$\vec{\nabla}.[N_i(\vec{v} + \vec{V}_i)] = K_i \tag{14}$$

- Energy conservation: This equation states that the divergence of the total energy flux (i.e., sum of the terms due to convection, diffusion and conduction) must be zero at every point.

$$\vec{\nabla}.(\rho\hat{H}\vec{v} + \sum_i N_i H_i \vec{V}_i - k\vec{\nabla}T) = 0$$
$$\hat{H} = \frac{1}{\rho}\sum_i N_i H_i \tag{15}$$

- Diffusion velocity: This velocity is given by Fick's law generalized to three dimensions and fro multiple-component systems,

$$\vec{V}_i = \frac{N^2}{N_i\rho}\sum_i M_i D_{ij}^* \vec{\nabla}\frac{N_j}{N} \tag{16}$$

- Equation of state: All gases are assumed to be ideal gas.

$$P = NRT \tag{17}$$

3-2- Soot Formation Model

Theoretically, as the flow increases, the luminous part of the flame gets longer until it extends beyond the boundary of the blue flame. With further increase in flow, unburned carbon dispersion may start at the top. This unburned carbon is formed within the flame and most of it burns as it travels to the tip of the flame. Experiments show that the more the turbulence of the flame, the more of the generated soot is burned through out the flame. In addition, nature of the fuel and combustion conditions affect dispersed solid carbon. For instance, increase of C/H ratio in hydrocarbons as well as increase in number of the braches (increased molecule compactness), increases the tendency of soot formation in the combustion process. Of other parameters that influence soot formation tendency significantly, is ambient pressure, i.e. soot formation decreases as the pressure increases. Luminosity of the flame is affected by flame temperature and soot. Since burning temperature of hydrocarbons are nearly the same, luminosity of the flame is a criterion for qualitative researches of soot formation [3].

The model which is used to predict soot formation is introduced in [9] for turbulent flames and it is assumed that soot is pure carbon. In this model, a single transport equation should be solved,

$$\frac{\partial}{\partial t}(\rho Y_{soot}) + \vec{\nabla}.(\rho \vec{v} Y_{soot}) = \vec{\nabla}.(\frac{\mu_t}{\sigma_{soot}} \vec{\nabla} Y_{soot}) + R_{soot} \quad (18)$$

where Y_{soot} is soot mass fraction, σ_{soot} is turbulent Prandtl number for soot transport, μ_t is turbulent viscosity and R_{soot} is net rate of soot formation (kg/m^3-sec).

R_{soot} is the balance of soot formation, $R_{soot,form}$, and soot combustion, $R_{soot,comb}$. Therefore,

$$R_{soot} = R_{soot,form} - R_{soot,comb} \quad (19)$$

The rate of soot formation is given by following empirical equation,

$$R_{soot,form} = C_s p_{fuel} \phi^r \exp(\frac{-E}{R_u T}) \quad (20)$$

where C_s is soot formation constant (kg/N-m-sec), p_{fuel} is fuel partial pressure, ϕ equivalence ratio, r is equivalence ratio exponent and E/R_u is activation temperature.

The rate of soot combustion is the minimum of two rate exponents.

$$R_{soot,comb} = \min[R_1, R_2] \quad (21)$$

$$R_1 = A' \rho Y_{soot} \frac{\varepsilon}{k}$$
$$R_2 = A' \rho \frac{Y_{ox}}{\nu_{soot}} \left(\frac{Y_{soot} \nu_{soot}}{Y_{soot} \nu_{soot} + Y_{fuel} \nu_{fuel}} \right) \frac{\varepsilon}{k} \quad (22)$$

In these equations, A' is called Magnusson constant, Y_{fuel} and Y_{soot} are mass fractions of oxidizer and fuel and ν_{fuel} and ν_{soot} are mass stiochiometries of oxidizer and fuel. Following values are suggested in these relations that are valid for variety of hydrocarbons.

Table 8- Constants on soot prediction model

Soot formation constant	Equivalence ratio exponent	Equivalence ration minimum	Equivalence ratio maximum	Activation temperature for soot formation rate	Magnusson constant for soot combustion
1.5	3	1.67	3	20000	4

The only constant that should be calculated in this model are mass stiochiometries for fuel and soot oxidation, which according to equation 3 and pure carbon burning equations are 3.4542 and 2.6667 respectively.

3-3- Flow Model

To determine whether the flow (which is caused by the candle flame) is laminar or turbulent, the problem was solved with both laminar and turbulent solvers and both methods indicated that the flow flied is laminar. Quantitative analysis to support this conclusion will be made later.

FLUENT is unable to predict soot formation in laminar models, because as mentioned in section 3-2, the model employed by FLUENT to predict soot formation holds only for turbulent flames. Hence, to estimate soot generation, one should use a turbulent flow model. The turbulent model which is chosen for this problem is two-equation k-ε model.

In this model turbulent kinetic energy, k ($= \overline{u_i'' u_i''}/2$), is obtained form its transport equation below.

$$\frac{D}{Dt}(\frac{1}{2}\overline{\rho u_i'' u_i''}) + \frac{\partial}{\partial x_k}[u_k''(\frac{1}{2}\overline{\rho u_i'' u_i''})] = -\overline{u_i''\frac{\partial p}{\partial x_i}} + \overline{u_i''\frac{\partial \tau_{ik}'}{\partial x_k}} - \overline{\rho u_i'' u_k''}\frac{\partial \tilde{u}_i}{\partial x_k} \quad (23)$$

Physical interpretation of each term in above equation is given in table 9.

Table 9- Physical interpretation of different terms is equation 23

$\frac{D}{Dt}(\frac{1}{2}\overline{\rho u_i'' u_i''})$	Rate of change of kinetic energy of turbulence
$\frac{\partial}{\partial x_k}[u_k''(\frac{1}{2}\overline{\rho u_i'' u_i''})]$	Kinetic energy of fluctuations convected by fluctuations (i.e., diffusion of fluctuation energy)
$\overline{u_i''\frac{\partial p}{\partial x_i}}$	Work due to turbulence
$\overline{u_i''\frac{\partial \tau_{ik}'}{\partial x_k}}$	Work of viscous stresses due to fluctuation motion
$-\overline{\rho u_i'' u_k''}\frac{\partial \tilde{u}_i}{\partial x_k}$	Production of turbulent stress and mean rate of strain: production of turbulent energy

By solving equation 23 to derive an expression for turbulent kinetic energy,

$$\overline{\rho}\widetilde{u}_j\frac{\partial k}{\partial x_j}=\frac{\partial}{\partial x_j}\left[\left(\frac{\mu_t}{\sigma_k}+\mu\right)\frac{\partial k}{\partial x_j}\right]-\overline{\rho}\overline{u_i''u_j''}\frac{\partial\widetilde{u}_i}{\partial x_j}-\frac{\mu_t}{\overline{\rho}^2}\frac{\partial\overline{\rho}}{\partial x_i}\frac{\partial\overline{p}}{\partial x_i}-\overline{\rho}\varepsilon \tag{24}$$

where σ_k is the turbulent Prandtl/Schmidt number for k and turbulent viscosity μ_t is,

$$\mu_t=C_\mu\overline{\rho}\frac{k^2}{\varepsilon} \tag{25}$$

and in above equation, C_μ is turbulence constant and ε is turbulent dissipation rate given by,

$$\rho\widetilde{u}_j\frac{\partial\varepsilon}{\partial x_j}=\frac{\partial}{\partial x_j}\left[\left(\frac{\mu_t}{\sigma_e}+\mu\right)\frac{\partial\varepsilon}{\partial x_j}\right]-C_{e1}\frac{\varepsilon}{k}(\overline{\rho}\overline{u_i''u_j''}\frac{\partial\widetilde{u}_i}{\partial x_j}-\frac{\mu_t}{\overline{\rho}^2}\frac{\partial\overline{\rho}}{\partial x_i}\frac{\partial\overline{p}}{\partial x_i})-C_{e2}\overline{\rho}\frac{\varepsilon^2}{k} \tag{26}$$

For these equations following constants are recommended [10].

$C_\mu=0.09$ $C_{e1}=1.44$ $C_{e2}=1.92$ $\sigma_k=1.0$ $\sigma_e=1.30$ $\sigma_t=0.7$

3-4- Flow Model Adaptation

As aforementioned, in order to predict soot formation in the flame with FLUENT, turbulent models should be used because of presence of $\vec{\nabla}.(\frac{\mu_t}{\sigma_{soot}}\vec{\nabla}Y_{soot})$ term in the soot transport equation. In [3] it is stated that soot combustion is merely resulted from turbulence effects in the flame. As it is seen in equations 21 and 22, soot combustion rate is minimum of two rate equations and the second rate equation depends upon turbulence dissipation rate. So, k-ε turbulence model should be adapted to this problem to eliminate effects of turbulence in the flow model (which are undesirable because of laminar nature of the flow) and to cancel out turbulence effects in the soot model. From equation 25 it is clear that if $C_\mu = 0$ then $\mu_t = 0$. Furthermore, if C_{e1} and C_{e2} go to zero, the turbulence dissipation rate equation will reduce to,

$$\rho\widetilde{u}_j\frac{\partial\varepsilon}{\partial x_j}=\frac{\partial}{\partial x_j}(\mu\frac{\partial\varepsilon}{\partial x_j}) \tag{27}$$

in which, μ is very small in comparison to other parameters and will reduce turbulence dissipation rate near enough to zero. This remedy in turns will reduce R_1 and R_2 to zero and this will also happen to $R_{comb,soot}$ in equation 21. There are three achievements in this technique: – the laminar nature of the flow in maintained in the turbulent model, – the turbulent soot prediction model can be used in FLUENT and – effects of soot combustion are nearly disappeared.

4- Preprocessing

4-1- Modeling and Grid Generation

The model and its dimensions and the grid generated in the enclosure are shown in figure 2.

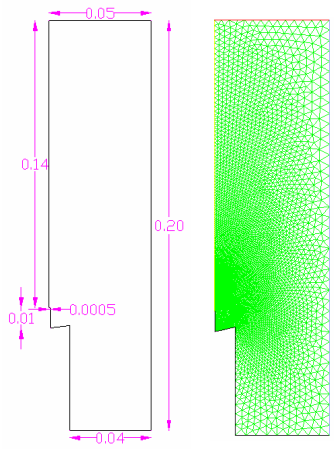

Figure 2- Model, dimensions and the grid

The candle of interest is assumed to be 0.02m in diameter whose top is slightly sloped due to melting effects and is placed in an enclosure with 0.2m height and 0.1m width. The candle height is 0.05m and the wick

length and wick diameter are 0.01m and 0.001m respectively. One full model and one symmetric model results indicated that symmetric assumption is a reasonable one. It is noticeable that the geometry of the candle is taken form [2] in which characteristics of n-eicosane flame are investigated experimentally and the results are used as inputs in this work.

In order to obtain more accurate results, 16532 cell zones become finer as they get closer to the wick. The fact that combustion reaction, species distribution and soot formation have extreme gradients across the flame implies the requirement of having very fine mesh in the vicinity of the flame.

4-2- Boundary Conditions

One crucial step of dealing the problem definition is obviously setting the boundary conditions. In this problem, some of the boundary conditions are quite easy to identify and some others require more attention.

- The wick tip is where the n-eicosane vapor diffuses into the air and mass fraction of fuel on this boundary is necessarily unity. Experiments which are reported in [10] indicate that temperature of n-eicosane vapor is slightly below boiling temperature (325^{o}C).
- The wick is divided into upper and lower segments. On the upper one, conditions are the same with wick tip. However, on the bottom segment temperature is slightly lower and there is very little chance for fuel to react [3].
- The temperature of the surface of the candle (which feeds the fuel to the wick) varies as measured more distant form the wick. The temperature of this region is set to wick bottom segment and decreases to reach melting pint of the fuel near the edge.
- The body of the candle as well as the floor of the enclosure has essentially the ambient temperature. Mass fraction of oxidizer on these boundaries is 0.21 as it is in air.
- The wall of the domain is where air flows through to reach the candle. This effect is modeled by use of a pressure inlet condition on which temperature is ambient temperature and oxygen mass fraction is 0.21.
- The ceiling of the enclosure is where the burned gases exit and conditions on it is the same as the wall except that this boundary is a pressure outlet in FLUENT literature.
- The last boundary is the axis. As noted before, axis is symmetry axis of the domain.

Figure 3 depicts the boundaries of the model.

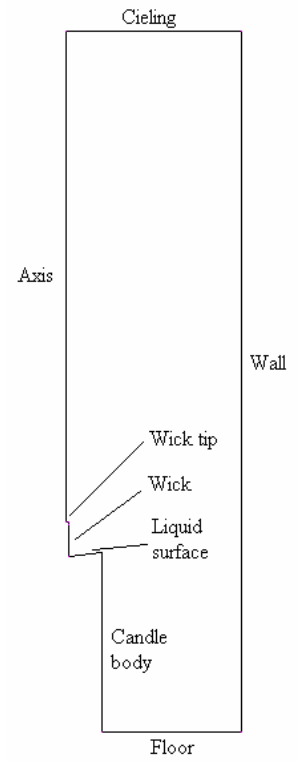

Figure 3- Boundaries of the model

5- Results

Figure 4 and 5 depict species mass fraction in the ambient air and reaction contour, flame temperature and soot generation respectively. Mass fraction contour for $C_{20}H_{42}$, O_2, CO_2 and H_2O are illustrated in figure 4. As it was expected, reaction in diffusion flames mainly takes place at a thin sheet (called flame sheet) and in middle parts of the flame there is almost no reaction. The flame sheet is the green surface started from the red region in the bottom to upward. The maximum flame temperature (which is illustrated in figure 5) is 1201K which is typical for hydrocarbons. As it is discussed in literature, sooting mainly occurs from tip of the flame and less than that from sides [3], this is clearly shown in the figure. It is remarkable that flame front is defined as locus of the points on which equivalence ratio is unity [11] and in figure 5, the flame front can be either determined form the location of the green sheet or from the location of maximum soot generation which is obviously the flame tip.

The velocity of gases above the wick is found to be of order 0.5m/sec which implies a Reynolds number of about 120 (assuming 1.225kg/m^3 for density and approximating the diameter of the jet with the wick's diameter). This Reynolds number is far less than critical value of 2000 for turbulent flames and it guaranties correctness of laminar flow assumption [1].

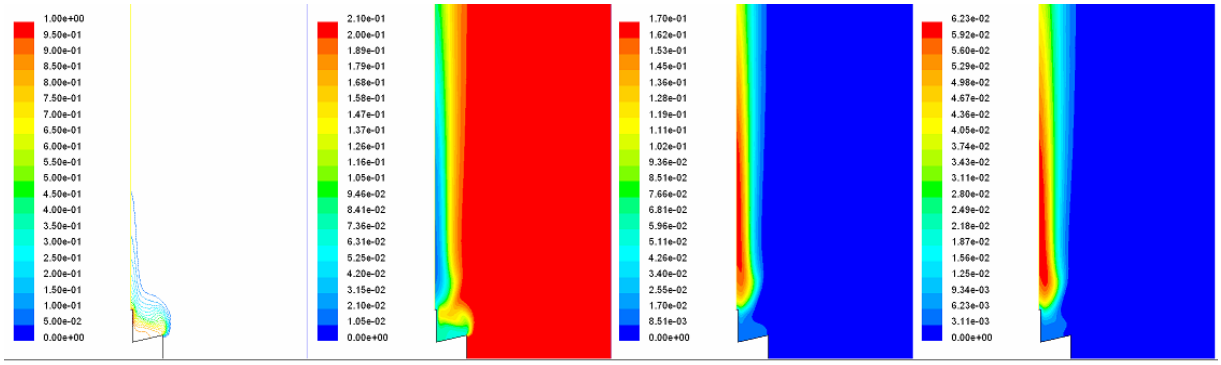

Figure 4- Contours of species mass fraction in atmospheric conditions, from left to right: n-eicosane, oxygen, carbon dioxide and water vapor

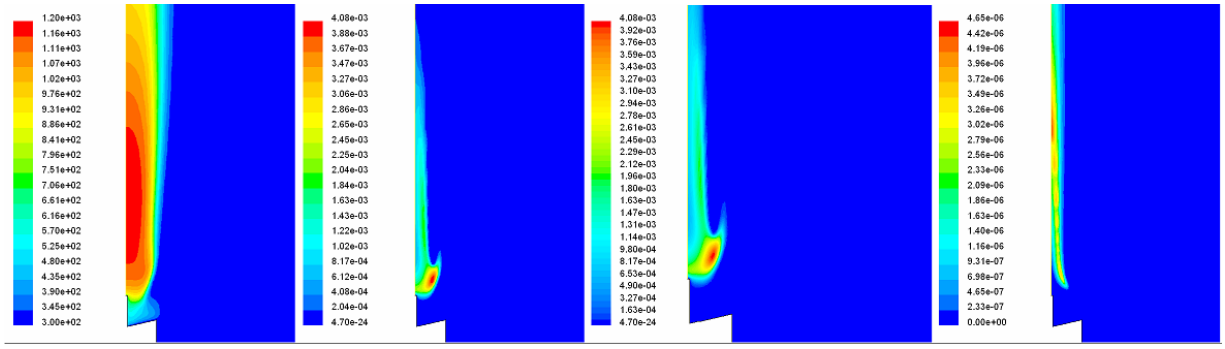

Figure 5- From left to right: - contour of temperature (K), - contour of reaction rate (kmole/m^3-sec), - closer view to the main reaction zone (flame sheet is colored in green) and - contour of soot generation (as was predicted most of the soot is dispersed from tip of the flame)

6- Effects of Ambient Pressure

Changes in the ambient pressure have significant effects on the flame properties. This influences become more interesting when the reaction rate does not depend on pressure directly (however it is indirectly related to the pressure though equation of state). Moreover, the mechanism model for this research is essentially independent of pressure. To investigate the reflection of the flame to the ambient pressure and to reason it is of interest in this research.

One must pay attention that diffusivities are inversely proportional to pressure; hence for each change in pressure, the values for diffusivities should be recalculated.

6-1- Effect of Pressure on Maximum Reaction Rate

Inverse relation of diffusion factors, which is the dominant phenomenon that brings fuel and oxygen into contact, with pressure causes excess amount of fuel entering the reaction region. This event, in turns, feeds more fuel into the reaction zone and increase in reaction rate in presence of sufficient oxygen. But further increase in the amount of fuel will results in retard of its own reaction [12]. Excessive reduction in the operating pressure (that will increase the fuel diffusion) can lead to flame disappearance. It is noticeable that trend of changes in n-eicosane maximum reaction rate as the pressure varies, has agreement with that of combustion of butane which is illustrated in [12]. Figure 6 shows the reaction contours for different pressures.

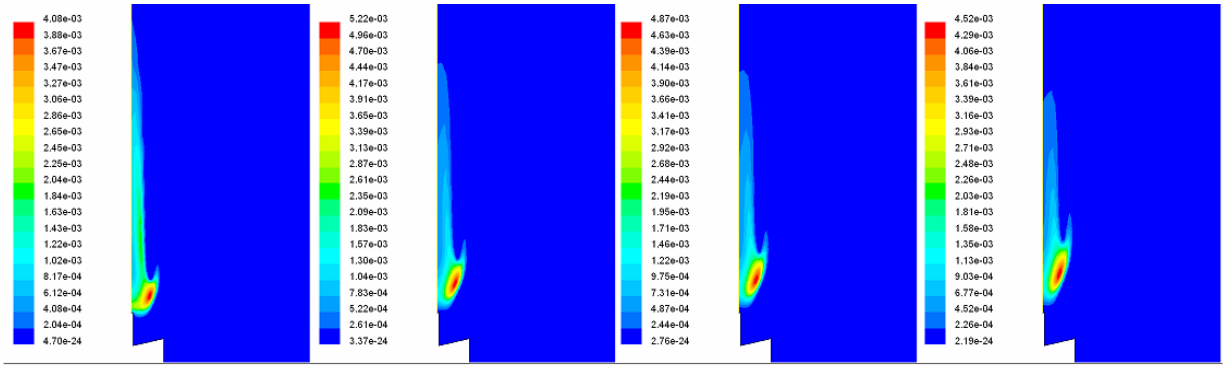

Figure 6- Contours of reaction rate (RR in kmole/m^3-sec) at different pressures. From left to right: - pr.=1atm, max(RR)=4.08e-3, - pr.=0.8atm, max(RR)= 5.22e-3, - pr.=0.7atm, max(RR)=4.87e-3 and - pr.=0.6atm, max(RR)=4.52e-3

The shortening in flame height and widening in flame width is verified qualitatively with the results of experiments reported in [1] (figure 7). The increase in flame width is obviously the result of increased molecular diffusion, which is the dominant phenomenon determining the flame width. The reduction in flame height is primarily due to increased flame sheet surface and reaction rate. Although more fuel is fed into the flame in lower pressures, extended reacting surface and higher reaction rate cause the fuel to burn more rapidly and its elevation is therefore lowered.

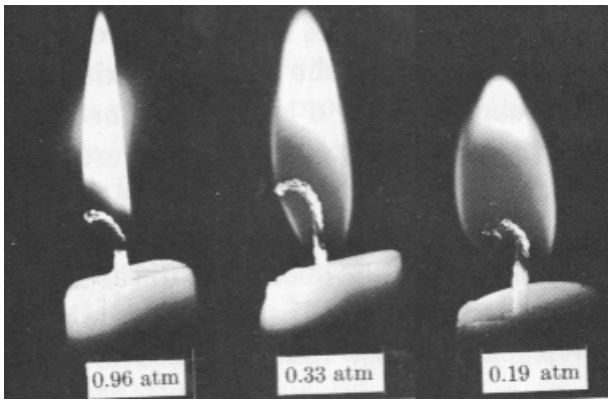

Figure 7- Changes in the candle flame front due to variations in operating pressure [1]

6-2- Effect of Pressure on Maximum Flame Temperature

Figure 8 illustrates changes in maximum flame temperature due to changes in ambient pressure. It can be noted that pressure does not have significant influence on the maximum flame temperature; however, it compacts the maximum temperature region. The compactness of this region is because reaction takes place at lower elevations and most of the heat of combustion is released there. Flame temperature in combustion reaction primarily depends upon nature of the reaction; i.e. reaction mechanism, fuel and oxidizer. Is this research the combustion mechanism is independent of pressure. This independency in reaction mechanism of pressure is quite general, for instance, four-step mechanism derived in [13] or eight-step global mechanism reported in [14] are also independent of pressure. The slight variation of flame temperature in different pressures is result of increase in reaction rate explained above.

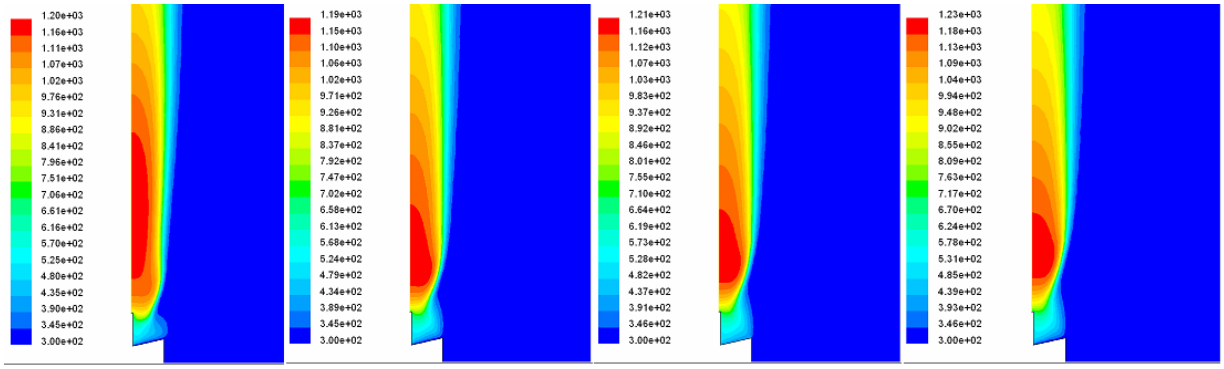

Figure 8- Contours of temperature (K) at different pressures. From left to right: - pr.=1atm, max(temp.)=1201, - pr.=0.8atm, max(temp)= 1194, - pr.=0.7atm, max(temp)=1210 and - pr.=0.6atm, max(temp)=1226

6-3- Effect of Pressure on Soot Emission

Experiments reported in [3] have shown that solid carbon generation in the diffusion flames decreases with reduction in operating pressure and at extremely low pressures there is almost no soot emission from the flame. While rising pressure from very low values, a luminous spot appears near the center of the flame. As it was noted earlier, luminosity of the flame is function of flame temperature and solid carbon and when temperature does not show significant variation with changes in pressure, luminous spot indicates soot formation zone. With further increase in operating pressure, the luminous region extends toward the tip of the flame. Results of this research depict this extension of soot (luminous zone) to the tip of the flame magnificently. But in quantitative point of view, numerical solution results show the opposite trend with experimental results. This mismatching is essentially due to unreliability of soot prediction model for quantitative analysis[5]. Figure 9 illustrates above explanations.

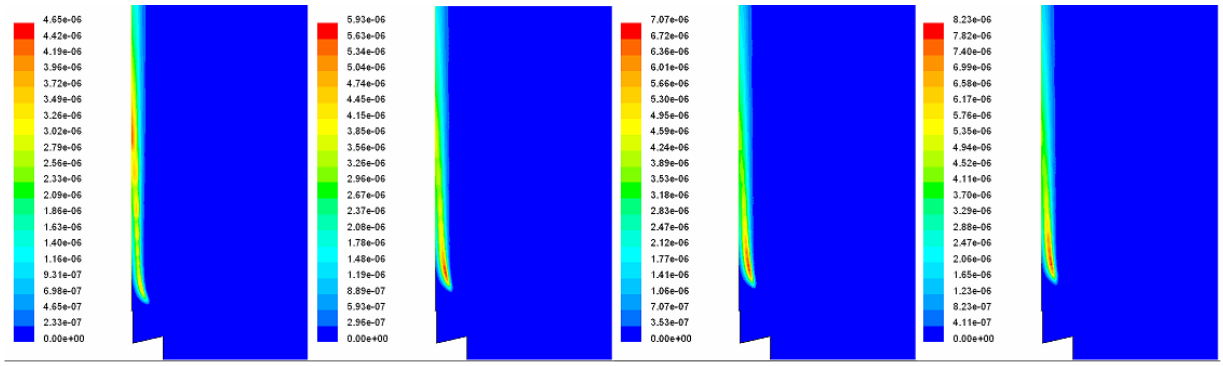

Figure 9- Contours of soot generation from the flame at different pressures (1atm, 0.8atm, 0.7atm and 0.6atm from left to right). Note that the red region in 1atm contour changes to yellow and extends to the sides in 0.8atm. In 0.7atm the yellow tip changes to green and the extension in the side reduces and in 0.6atm most of the soot in generated from the side of the flame.

7- Summary and Conclusion

Primary goal of present work was to perform a fundamental research on laminar diffusion flame of a candle to gain better insight into the process itself and the parameters that affect it, through modeling, investigating and reasoning the results.

Among numerous fuels that candles are produced from, n-eicosane is known as the most frequently paraffin used in candles manufacturing. Thermo-chemical properties of the fuel were then tabulated. Due to extreme sensitivity of combustion reaction to thermo-physical properties of species, standard methods to estimate these properties accurately were employed. Model of the reaction mechanism and mathematical model of physical aspects and dynamics of the problem were reviewed as set of equations that need to be solved. The sample candle and enclosure geometry as well as proper boundary conditions were described as the final step of preprocessing.

---

5 The detailed chemistry and physics of soot formation are quite complex and only approximated by models used by FLUENT. In use of these models, one should consider the results only qualitative indicator of the system performance [15].

Occurrence of reaction at the flame sheet in diffusion flames was illustrated and compared to the theory of diffusion flames. Experiments show that solid carbon is released mainly through tip of the flame; this aspect is depicted in the numerical solution results. Operating pressure was then changed to examine response of the flame.

- It was found that reaction rate increase as the pressure decreases, but further decrease in pressure results in decrease of the reaction rate until the flame goes off.
- The width of the flame was shortened as the pressure was reduced and in contrast its height was increased as a result of enlargement in flame sheet surface and higher reaction rate.
- Maximum flame temperature did not show significant changes in indifferent pressures; however, the region in which the flame temperature is maximum, was shortened in lower pressure due to shortening in reaction zone extension.
- In reduced pressures, soot concentration increased in lower part of the flame; i.e., the maximum soot concentration moved from tip of the flame downward as the pressure was fallen. This can be one of the reasons that luminous part of the flame moves down as the pressure decreases, because luminosity is known to be dependent upon temperature and solid carbon generation in the flame.

Acknowledgement

Authors wish to express their gratefulness to them who helped us in gathering information resources used in the presented work: Mr. Behrouz Abbasi, Mr. Arash Moharreri and Mr. Iman Roohi.

References

1- Fristrom, R. M. and Westenberg, A. A., “Flame Structure”, McGraw-Hill, 1965.
2- Burge, S. J. and Tipper, F. H., "The Burning of Polymers", Combustion and Flame, vol. 13, pp. 495-505, 1969.
3- Gaydon, A. G., and Wolfhard, H. G., “Flames: Their Structure, Radiation and Temperature”, Chapman and Hall, 3rd edition, 1970.
4- Williams, Allan, "The Mechanism of Combustion of Droplets and Sprays of Liquid Fuels", Oxidation and Combustion Reviews, Elsevier Publishing Company, pp. 3-45, 1968.
5- "The Heat of Combustion of Candle Paraffin", Louisiana State University Department of Chemistry, 1996.
6- Matthai, M. and Petereir, N., "The Quality Candle", 2004.
7- Perry, Robert H. and Green, Don W., "Perry's Chemical Engineers Handbook", McGraw Hill, 1999.
8- Westbrook, C. K. and Dryer F. L. "Chemical Kinetic Modeling of Hydrocarbons Combustion", Progress in Energy and Combustion Science, 10: 1-57, 1384.
9- Khan, I. M. and Greeves, G., "A Method for Calculating the Formation and Combustion of Soot in Diesel Engines", Heat Transfer in Flames, chapter 25, Washington DC, 1974.
10- Kuo, K. K., “Principles of Combustion”, John Wiley and Sons, 1986.
11- Turns, S.R., and Mantel, S.J., "An Introduction to Combustion", McGraw Hill, 2000.
12- Minkoff, G. J. and Tipper, F. H., "Chemistry of Combustion Reaction", London Butterworth, 1962.
13- Hautman, D. J. and Dryer, F. L. and Glassman, I., "Simplified Reaction Mechanism for Oxidation of Hydrocarbon Fuels in Flames", Combustion Science and Technology, vol. 25, pp. 219-235, 1981.
14- Glassman, I., "Combustion", Academic Press, 3rd edition, 1996.
15- FLUENT® v. 6.1 Documentation.